Spatial Pattern and Zonal Shift of the North Atlantic Oscillation. Part I: A Dynamical Interpretation

Dehai Luo and Zhihui Zhu

Physical Oceanography Laboratory, College of Physical and Environmental Oceanography,
Ocean University of China, Qingdao, China

Rongcai Ren

LASG, Institute of Atmospheric Physics, Chinese Academy of Sciences, Beijing, China

Linhao Zhong

LACS, Institute of Atmospheric Physics, Chinese Academy of Sciences, Beijing, China

Chunzai Wang

NOAA/Atlantic Oceanographic and Meteorological Laboratory, Miami, Florida

(Manuscript received 2 October 2009, in final form 12 April 2010)

ABSTRACT

This paper presents a possible dynamical explanation for why the North Atlantic Oscillation (NAO) pattern exhibits an eastward shift from the period 1958–77 (P1) to the period 1978–97 (P2) or 1998–2007 (P3). First, the empirical orthogonal function analysis of winter mean geopotential heights during P1, P2, and P3 reveals that the NAO dipole anomaly exhibits a northwest–southeast (NW–SE) tilting during P1 but a northeast–southwest (NE–SW) tilting during P2 and P3. The NAO pattern, especially its northern center, undergoes a more pronounced eastward shift from P1 to P2. The composite calculation of NAO events during P1 and P2 also indicates that the negative (positive) NAO phase dipole anomaly can indeed exhibit such a NW–SE (NE–SW) tilting. Second, a linear Rossby wave formula derived in a slowly varying basic flow with a meridional shear is used to qualitatively show that the zonal phase speed of the NAO dipole anomaly is larger (smaller) in higher latitudes and smaller (larger) in lower latitudes during the life cycle of the positive (negative) NAO phases because the core of the Atlantic jet is shifted to the north (south). Such a phase speed distribution tends to cause the different movement speeds of the NAO dipole anomaly at different latitudes, thus resulting in the different spatial tilting of the NAO dipole anomaly depending on the phase of the NAO. The zonal displacement of the northern center of the NAO pattern appears to be more pronounced because the change of the mean flow between two phases of the NAO is more distinct in higher latitudes than in lower latitudes.

In addition, a weakly nonlinear analytical solution, based on the assumption of the scale separation between the NAO anomaly and transient synoptic-scale waves, is used to demonstrate that an eastward shift of the Atlantic storm-track eddy activity that is associated with the eastward extension of the Atlantic jet stream is a possible cause of the whole eastward shift of the center of action of the NAO pattern during P2/P3.

1. Introduction

The North Atlantic Oscillation (NAO) is one of the most prominent low-frequency modes confined in the Atlantic basin over the Northern Hemisphere (NH) (Walker 1924; Wallace 2000). In the past decades, the impact of the NAO has attracted increasing scientific interest because the NAO exerts an important impact on the regional climate and weather in the North Atlantic region and adjacent continents and on oceanic circulations in the Atlantic basin (Cayan 1992; Hurrell 1995a; Visbeck et al. 1998). Although the sea surface temperature (SST) anomalies in the Atlantic region can

Corresponding author address: Dr. Dehai Luo, College of Physical and Environmental Oceanography, Ocean University of China, Qingdao 266003, China.
E-mail: ldh@ouc.edu.cn

modulate the NAO patterns (Li et al. 2007), the inherent time scale of the NAO events is found to be about two weeks (Feldstein 2003; Benedict et al. 2004; Franzke et al. 2004), which has been confirmed by Luo et al. (2007a) in a weakly nonlinear NAO model. In recent years, many investigations have found an eastward shift of the center of action of the NAO from the period 1958–77 (P1) to the period 1978–97 (P2) (Hilmer and Jung 2000; Jung and Hilmer 2001; Jung et al. 2003; Johnson et al. 2008). This eastward shift tends to result in a significant increase in the correlation between the NAO index and the sea ice export from the Arctic region to the open Atlantic through Fram Strait (Hilmer and Jung 2000; Jung and Hilmer 2001).

The physical cause of the eastward shift of the centers of action of the NAO patterns during P2 has been widely investigated by using observational data and numerical models since this phenomenon was detected in 2000. In a coupled ECHAM–OPYC3 model, increasing greenhouse gas concentrations are found to be the main cause for the eastward shift of the center of action of the observed NAO pattern (Ulbrich and Christoph 1999). Peterson et al. (2002) noted that this eastward shift may be due to an increase in the strength of the mean westerly wind in the Atlantic basin. But in a numerical model, Peterson et al. (2003) further found that the spatial pattern of the NAO exhibits a nonlinear dependence on the NAO index, which is shifted to the east (west) for the high (low) index, and they concluded that the eastward shift of the NAO might be attributed to the transition from a negative (during P1) to positive NAO phase (during P2). Cassou et al. (2004) used a cluster analysis to find that the apparent shift in the NAO position might result from the dominance of an intrinsically more eastward displaced positive NAO phase. In a weakly nonlinear NAO model, Luo and Gong (2006) confirmed that in a strong mean westerly wind the mean flow-induced eastward shift of the NAO will exceed the eddy-induced westward shift, and thus the center of action of the NAO pattern undergoes an eastward shift during P2. Using the method of self-organizing maps Johnson et al. (2008) recently found that the secular eastward shift may be understood as a change in dominance from the westward-displaced and negative NAO-like patterns to the eastward-displaced and positive NAO-like patterns.

Although many previous studies are focused on the possible cause of the eastward shift of the center of action of the NAO pattern during P2 (e.g., Peterson et al. 2002; Jung et al. 2003; Luo and Gong 2006), the physical mechanisms of the eastward shift of the center of action of the NAO pattern are not clear yet. In particular, why the NAO patterns can have different spatial patterns for the different phases is still an unsolved and important problem. In this paper, we will address these problems from observational and theoretical aspects and will present a possible dynamical explanation of why the center of action of the NAO pattern can undergo an eastward displacement during P2.

The paper is organized as follows. In section 2, we will present observational results to show that the NAO pattern for the positive (negative) phase is a northeast–southwest (northwest–southeast) tilted dipole anomaly and the center of action of the NAO pattern, especially its north center, undergoes a pronounced eastward shift during P2 as compared with during P1. In section 3, we will provide a likely explanation of why the positive and negative phases of the NAO have different spatial patterns, based on both the meridional distribution of the Atlantic jet stream during the NAO life cycle and the linear Rossby wave formula in a slowly varying media. Section 4 is devoted to present a possible link of the eastward shift of the center of action of the NAO pattern with the eastward displacement of the Atlantic storm-track eddy activity associated with the eastward extension of the Atlantic jet stream during P2. In this section, a weakly nonlinear NAO model developed by Luo et al. (2007a,b) is also used to interpret why the eastward shift of the Atlantic storm-track eddy activity is able to cause the eastward shift of the centers of action of the NAO patterns during P2. Finally section 5 provides conclusions and discussion.

2. NAO patterns and eastward shift

The data used in the present study are from National Centers for Environmental Prediction–National Center for Atmospheric Research (NCEP–NCAR) reanalysis. Variables analyzed include the monthly mean sea level pressure (SLP) and the daily geopotential heights and winds from December 1958 to December 2007. The data are on a $2.5° \times 2.5°$ latitude–longitude grid.

As in Johnson et al. (2008), we subdivide the data into three periods: 1958–77 (P1), 1978–97 (P2), and 1998–2007 (P3). Here P1 and P2 are identical to those of previous works (Hilmer and Jung 2000; Peterson et al. 2003), but P3 corresponds to a more recent period during which the NAO index experienced a transition of more neutral values than P2 (Overland and Wang 2005; Johnson et al. 2008).

Figure 1 shows the first empirical orthogonal function (EOF) modes of NH winter [December–February (DJF)] mean SLP anomalies in the Atlantic basin during P1, P2, and P3. It is found that a marked difference exists between P1 and P2/P3 for the NAO-related winter mean SLP anomalies even though the difference of the NAO pattern between P3 and P2 is smaller except its sign. The NAO pattern exhibits a northwest–southeast tilted dipole anomaly during P1 (Fig. 1a), but a northeast–southwest
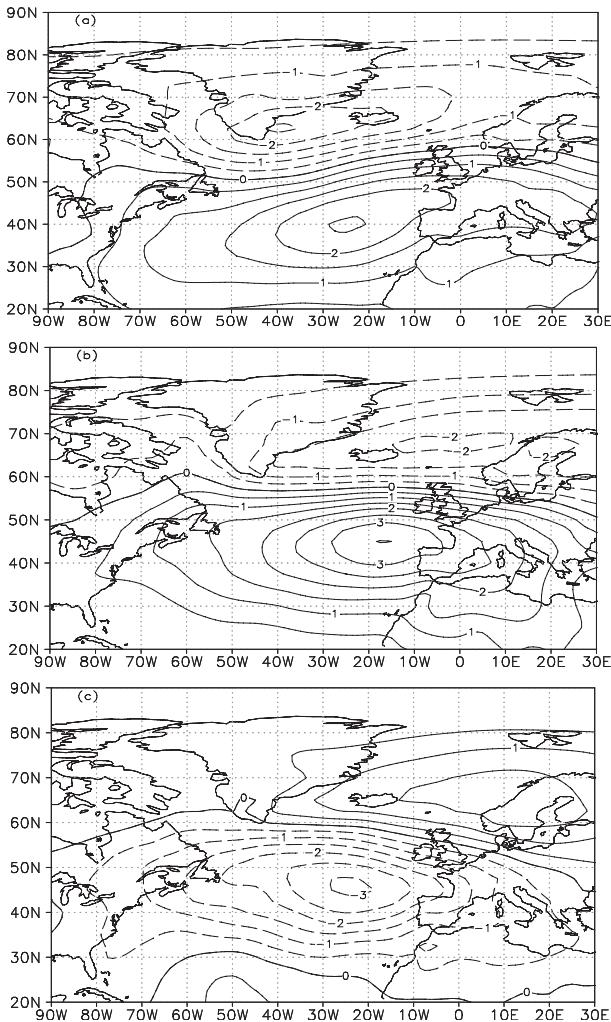
FIG. 1. First EOF of wintertime (DJF) North Atlantic SLP anomalies (hPa) for three periods: (a) 1958–77 (P1), (b) 1978–97 (P2), and (c) 1998–2007 (P3). The first EOF explains (a) 42.6%, (b) 49.2%, and (c) 42.1%.

tilted dipole anomaly during P2 and P3 (Figs. 1b,c). Moreover, the NAO pattern is found to undergo a whole eastward shift from P1 to P2. This result is also consistent with the previous findings (Hilmer and Jung 2000; Jung et al. 2003; Peterson et al. 2003). In particular, the eastward shift is found not to be an artifact of changes in observational practices, which has been further confirmed by Jung et al. (2003) by calculating the leading EOFs from the linearly detrended data and the SLP anomalies regressed into the normalized NAO index. Further, we can see from Fig. 1 that the northern center of the NAO pattern seems to undergo a distinct eastward shift of about 40° longitude from P1 to P2, while the zonal shift of its southern center is only of about 10° longitude. Although the NAO pattern during P3 looks like that during P2, the eastward shift of its northern

center is likely to be more pronounced during P3 than during P2. Because the purpose of this paper is to investigate what causes the whole eastward shift of the NAO centers of action from the negative to positive phase period, the composite that we perform in the next section is mainly focused on the spatial structures of NAO events during P1 and P2.

Since the EOFs are sensitive to the sampling (Cheng et al. 1995), Jung et al. (2003) concluded that the eastward shift of the NAO pattern may be due to the sampling variability of the leading EOF. Recently, Franzke (2009) noted that the NAO index may not exhibit a statistically significant trend by applying the empirical mode decomposition (EMD) method. Obviously, this may be related to the use of the different statistical method. It has, however, been widely recognized that the NAO pattern does indeed undergo an eastward shift from P1 to P2, which may result from increasing greenhouse gas concentrations and an increase in the strength of the mean westerly wind in the North Atlantic regions (Ulbrich and Christoph 1999; Peterson et al. 2003; Johnson et al. 2008). Such an eastward shift is really statistically significant (Jung et al. 2003; Peterson et al. 2003), which can also be confirmed by calculating the rotated EOFs (not shown) in that the rotated EOFs are less sensitive to the sampling (not shown). Numerical experiments using the GCM indicate that the Atlantic storm-track eddy activity exhibits a downstream intensification under the CO_2 doubling condition (Hall et al. 1994). Thus, it is possible that the whole eastward shift of the NAO pattern is related to the downstream displacement of the Atlantic storm-track eddy activity associated with the eastward extension of the Atlantic jet in a warmer climate (Ulbrich and Christoph 1999; Sigmond et al. 2004). Further, we propose a hypothesis that the different spatial structure of the NAO pattern may be, to a large extent, dominated by the different meridional distributions of the westerly jet for the different phases of the NAO. To test this hypothesis, the composite of geopotential height and wind fields for the selected NAO events based on the daily NAO index is presented in the following sections.

3. Spatial structure of the composite NAO pattern and its dynamical explanation

To see whether the NAO variability in the EOF fields shown in Fig. 1 is true and whether the spatial pattern of the NAO depends on its phase, here we present the composites of the geopotential height anomalies for the different phases of the NAO. Figure 2 shows the composite of the geopotential height anomalies at 250 mb for positive/negative NAO events during P1 based on the daily NAO index presented by Benedict et al. (2004). An

(a)
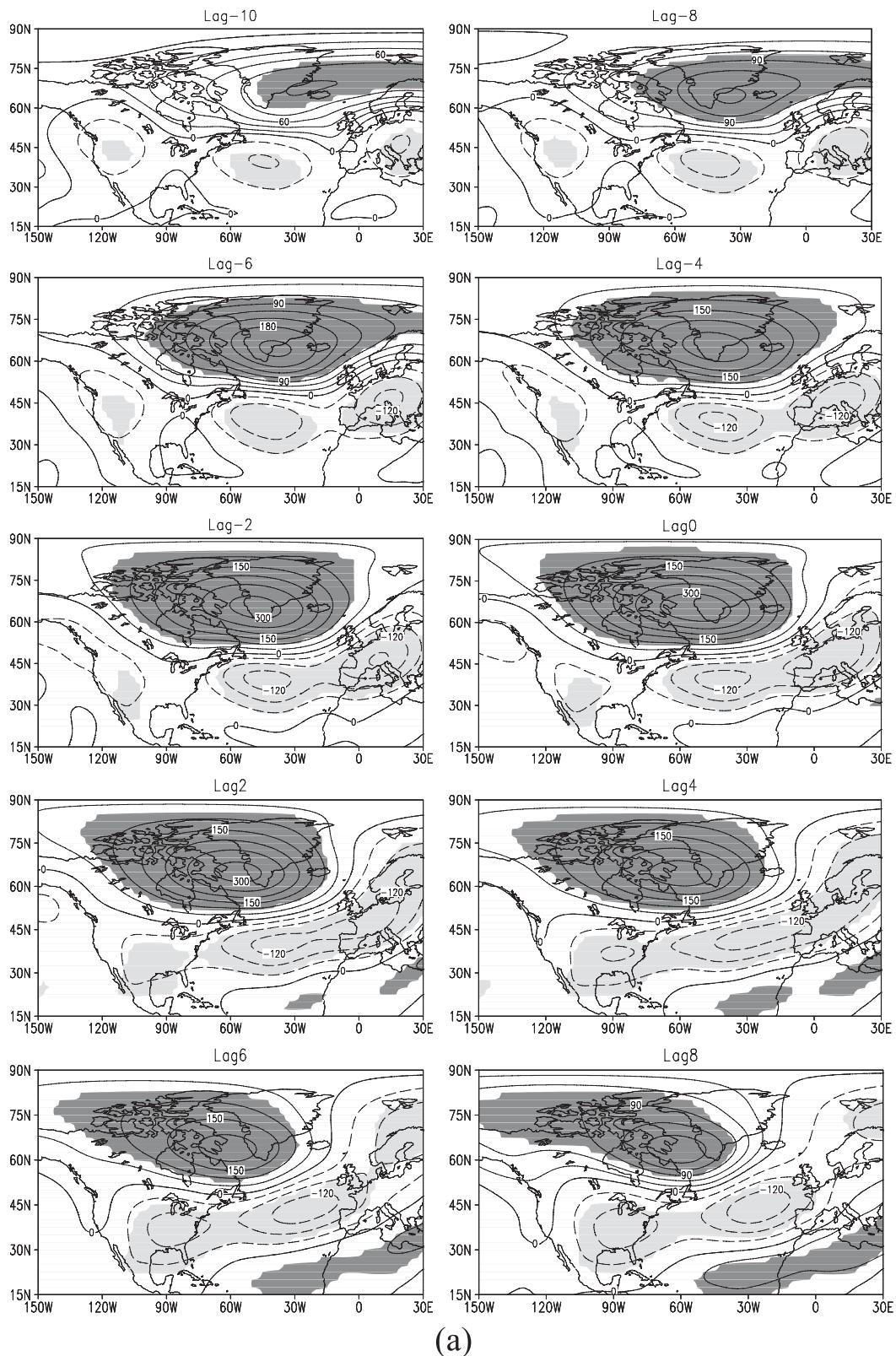
FIG. 2. Composites of the geopotential height anomalies at 250 mb for positive and negative phase NAO events during 1958–1977 (P1) based on the daily NAO index presented by Benedict et al. (2004). The solid and dashed lines represent the positive and negative anomalies, respectively, and the dark (light) shading indicates positive (negative) t values that exceed the 95% confidence level.
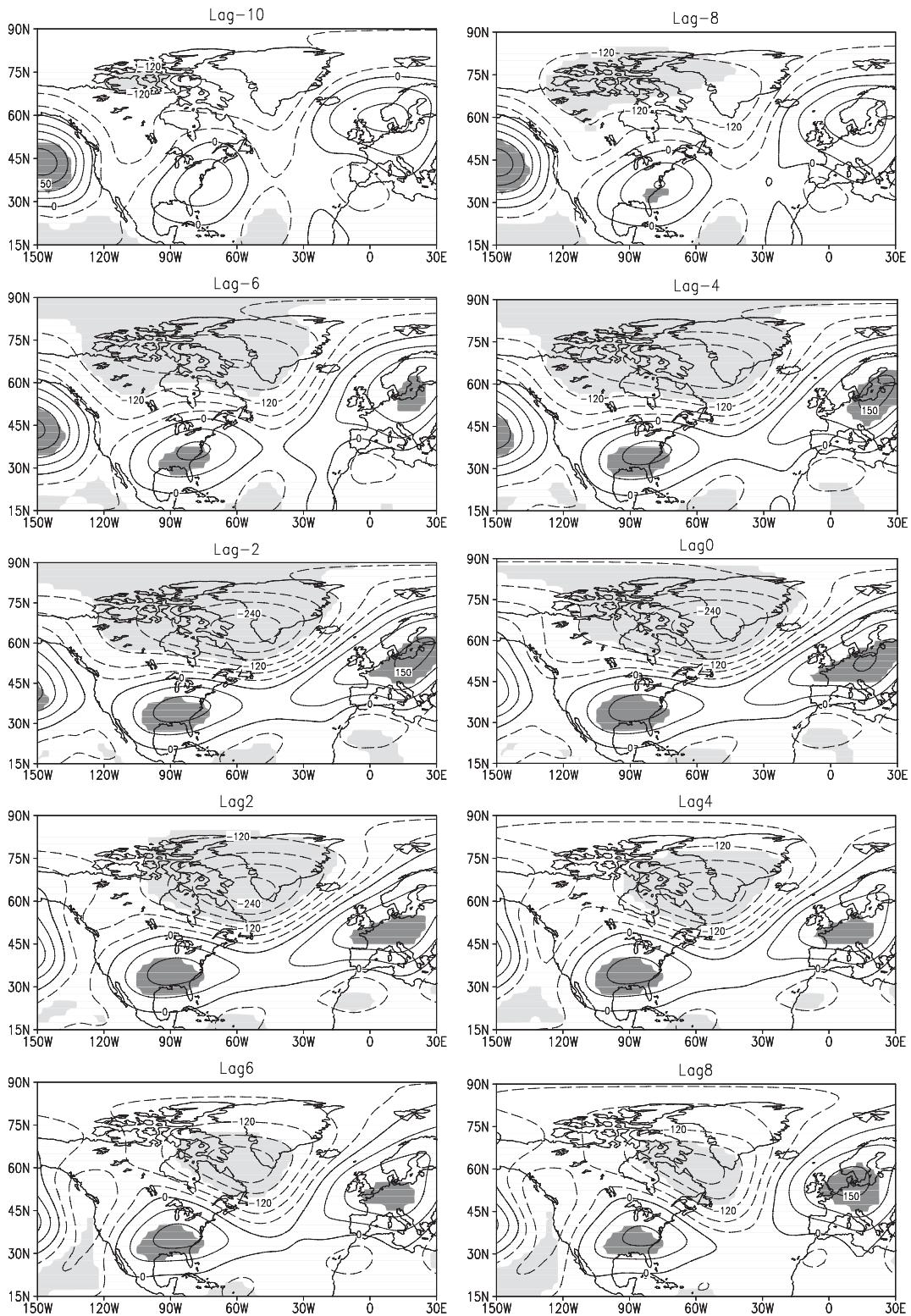
(b)

FIG. 2. (*Continued*) Shown are the (a) negative and (b) positive NAO phases. Lag 0 is defined to be the day on which the NAO index is at its largest value. Negative (positive) lags represent days before (after) lag 0.

event is specified as a string of four or more consecutive days in which the NAO index is greater than 1.33 standard deviations (Benedict et al. 2004). In a composite, lag 0 is defined to be the day on which the index is at its largest value. The composites, shown in Fig. 2, are all statistically significant at the 95% confidence level (Feldstein 2003; Feldstein and Franzke 2006). It is seen that during P1 the positive (negative) phase NAO pattern exhibits a NE–SW (NW–SE) tilted dipole anomaly. Since negative phase NAO events are dominant during P1, it is inevitable that the first EOF pattern during P1, as shown in Fig. 1, exhibits a northwest–southeast tilted dipole. Figure 3 shows the composites of positive and negative NAO events during P2. It is also seen that during P2 the NAO pattern for the positive (negative) phase still displays a northeast–southwest (northwest–southeast) tilted dipole structure. This suggests that the spatial structure of the NAO pattern is dependent on its phase. Because positive (negative) phase NAO events are dominant during P2 (P1), the winter mean EOF pattern of the NAO during P2 (P1) has a NE–SW (NW–SE) tilted dipole structure. At the same time, the difference in the NAO patterns between P2 and P1 is also statistically significant at the 95% confidence level (not shown). A comparison of the composited NAO anomaly field between P1 and P2 shows that the NAO centers of action for both positive and negative phases exhibit a whole eastward shift from P1 to P2. The result of the composite field is consistent with that of the EOF field, thus confirming the eastward shift of the NAO pattern from P1 to P2.

To reveal the possible cause of why the spatial structure of the NAO depends on its phase, we present the composites of zonal mean winds at 250 mb for the positive and negative phase NAO events during P1 and P2 in Fig. 4. It is interesting to see that there is a northward (southward) shift of the jet stream core in the Atlantic basin for the positive (negative) phase of the NAO. In particular, the Atlantic jet is more intense for the positive phase than for the negative phase. Thus, it can be inferred that the difference of the Atlantic jet stream between the positive and negative NAO phases may lead to the distinction of the spatial structures of the NAO pattern between two phases. Although the NAO is a nonlinear problem, as a first-order approximation the zonal movement of the NAO anomaly can be at least described by the linear theory of a Rossby dipole wave. Here we will use the propagation theory of the linear Rossby wave in a slowly varying basic flow with a meridional shear developed by Hoskins and Karoly (1981) and Yang and Hoskins (1996) to elucidate a possible mechanism of the spatial tilting of the NAO pattern.

For a nondivergent atmosphere, the barotropic vorticity equation linearized about a basic state $U(y)$ that has a meridional shear can be obtained as

$$\left(\frac{\partial}{\partial t} + U\frac{\partial}{\partial x}\right)\nabla^2\psi' + (\beta - U'')\frac{\partial\psi'}{\partial x} = 0, \tag{1}$$

where $U'' = \partial^2 U/\partial y^2$ and β is the meridional gradient of the Coriolis parameter centered at a given latitude ϕ_0. Note that Eq. (1) has no boundary condition in an infinite β plane but has a periodic boundary in the zonal direction and a rigid boundary in the meridional direction in a β-plane channel.

Here we assume that the sheared basic flow is a slowly varying inhomogenous media if the latitudinal variation of the sheared basic flow is not very strong. In such an inhomogeneous media, the amplitude, wavenumber, and frequency of the wave are slowly varying. In this case, the Wentzel–Kramers–Brillouin (WKB) method can be used to obtain the dispersion relation of a linear Rossby wave in a slowly varying sheared basic flow (Hoskins and Karoly 1981; Branstator 1983; Hoskins and Ambrizzi 1993; Yang and Hoskins 1996). Assuming that the wave solution for Eq. (1) is $\psi' = Ae^{i\theta}$ in which A is the wave amplitude, $i = \sqrt{-1}$, and $\theta = kx + my - \omega t$ is the wave phase, we can obtain (Hoskins and Ambrizzi 1993; Yang and Hoskins 1996)

$$\omega = Uk - \frac{k(\beta - U'')}{k^2 + m^2}, \tag{2a}$$

$$C_{gx} = \frac{\partial\omega}{\partial k} = U + \frac{(k^2 - m^2)(\beta - U'')}{(k^2 + m^2)^2}, \tag{2b}$$

$$C_{gy} = \frac{\partial\omega}{\partial m} = \frac{2km(\beta - U'')}{(k^2 + m^2)^2}, \tag{2c}$$

$$\frac{D_g\omega}{Dt} = 0, \tag{2d}$$

$$\frac{D_g k}{Dt} = 0, \tag{2e}$$

and

$$\frac{D_g m}{Dt} = \frac{k}{(k^2 + m^2)}\frac{\partial(\beta - U'')}{\partial y} - k\frac{\partial U}{\partial y}, \tag{2f}$$

where

$$\frac{D_g}{Dt} = \frac{\partial}{\partial t} + C_{gx}\frac{\partial}{\partial x} + C_{gy}\frac{\partial}{\partial y}.$$

It is evident that the frequency and the zonal wavenumber of the linear Rossby wave are conserved, but the meridional wavenumber can be varied because $U(y)$ is varying in the meridional direction.

As pointed out by Hoskins and Ambrizzi (1993), despite the probable violation of the condition for the strict validity of the theory, it can at least qualitatively be used to understand the observations and model results. In past decades, the linear theory of barotropic Rossby wave propagation in a slowly varying media was widely used to investigate the energy propagation of quasi-stationary ($\omega \approx 0$) or stationary ($\omega = 0$) waves by looking at the ray-tracing path of the group velocity of these waves (Hoskins and Karoly 1981; Branstator 1983; Hoskins and Ambrizzi 1993; Yang and Hoskins 1996). Because we are mainly interested in the movement tendency of a NAO dipole anomaly, rather than its energy propagation, Eq. (2a) is only used here. Also, it is seen that we can have $D_g m/Dt \approx 0$ from Eq. (2f) when k is rather small and when $U(y)$ is slowly varying. This condition is approximately satisfied in a slowly varying flow with a latitudinal variation in that the NAO pattern has a low zonal wavenumber.

Although the above formula is obtained based on the linear theory in slowly varying media, $c_x = \omega/k$ can be used to identify how the wave packet moves in the zonal (x) direction (Yang and Hoskins 1996). In fact,

$$c_x = U - \frac{(\beta - U'')}{k^2 + m^2}$$

is still correct at least as the first-order approximation of the linear Rossby wave equation in a β-plane channel if $U(y)$ is slowly varying. This formula can be easily derived by the perturbation expansion of the linear barotropic Rossby wave equation in a β-plane channel.

In this paper, the energy propagation of a wave packet is not the main aim of the present paper because the paper is focused on qualitatively understanding how the phase speed of a wave packet depends on the latitudinal distribution of the basic flow. Thus, it is at least reasonable to use $c_x = \omega/k$ to qualitatively examine the latitudinal distribution of the phase speed of the NAO pattern with the background flow as the first-order approximation. This can also be confirmed by numerical solutions presented in Luo et al. (2010, hereafter Part II).

Here, we choose parameters $k = 2/(a_0 \cos\varphi_0)$ ($a_0 = 6371$ km) and $m = \pm 2\pi/L_y$ as the zonal and meridional wavenumbers of the NAO dipole anomaly, respectively. Given φ_0 and L_y, $c_x(y)$ can be calculated by using $U(y)$ in Fig. 4. For $\varphi_0 = 45°$N and $L_y = 5000$ km, the zonal phase speed $C(y) = c_x(y)$ of the NAO dipole anomaly for its two phases for the observed basic flows, as shown in Fig. 4, is shown in Fig. 5.

It is found that for the positive (negative) phase the Rossby dipole mode moves faster (slower) in the higher latitudes than in the lower latitudes because the jet core

shifts toward the north (south) during its life cycle. Thus, it is inevitable that during P1 and P2 the positive (negative) NAO dipole anomalies exhibit a NE–SW (NW–SE) tilting. This can probably explain why the positive and negative NAO patterns in Figs. 2 and 3 can have different spatial structures. However, it must be pointed out that, although the phase speed of the linear Rossby dipole wave is larger in higher (lower) latitudes for the positive (negative) phase (Fig. 5 at lag 0), the movement speed of the observed NAO anomaly may not be so large. This is because the eddy-driven NAO anomaly itself can produce a westward movement speed to counteract the eastward phase speed of the NAO anomaly (linear Rossby dipole wave part) induced by the background flow (Luo and Gong 2006). Of course, the different spatial patterns of the positive and negative phases can also be explained by the highly idealized schematic pictures for the different NAO phases shown in Fig. 6, which are plotted in terms of a weakly nonlinear NAO model (Luo et al. 2007b). As demonstrated by Luo et al. (2007b), in a preexisting uniform westerly wind, a dipole mode resembling the positive (negative) NAO anomaly can be excited by transient synoptic-scale eddies if the planetary- and synoptic-scale waves prior to the NAO can match in a moderate parameter range. The interaction between the amplified positive (negative) NAO dipole anomaly and a topographic monopole wave anomaly can excite a westerly jet anomaly in midlatitudes and make the excited westerly jet anomaly shift to the north (south) for the positive (negative) phase. According to the meridional distribution of the zonal phase speed of the linear Rossby wave shown in Fig. 5, it is concluded that the positive (negative) phase NAO dipole anomaly inevitably exhibits a NE–SW (NW–SE) tilted dipole structure. Thus, it is likely that the different spatial patterns of the positive and negative NAO phases result from the different meridional distributions of the Atlantic jets associated with the positive and negative phase NAO events. Benedict et al. (2004) noted that the different spatial pattern of the NAO anomaly for its different phase is more likely to be attributed to the different type of wave breaking (Thorncroft et al. 1993; Franzke et al. 2004). In this process, the anticyclonic or cyclonic wave breaking is characterized by a southwest–northeast or northwest–southeast tilted trough–ridge pair. However, in our analytical model (Luo et al. 2007a) and in the numerical simulation presented in Part II, the cyclonic (anticyclonic) wave breaking can still be seen for the negative (positive) phase even though the eddy-driven NAO dipole anomaly is zonally symmetric. Thus, the wave breaking is not the only cause of the NAO tilting; instead the NE–SW (NW–SE) tilting of the NAO pattern for the positive (negative) phase is more likely to be
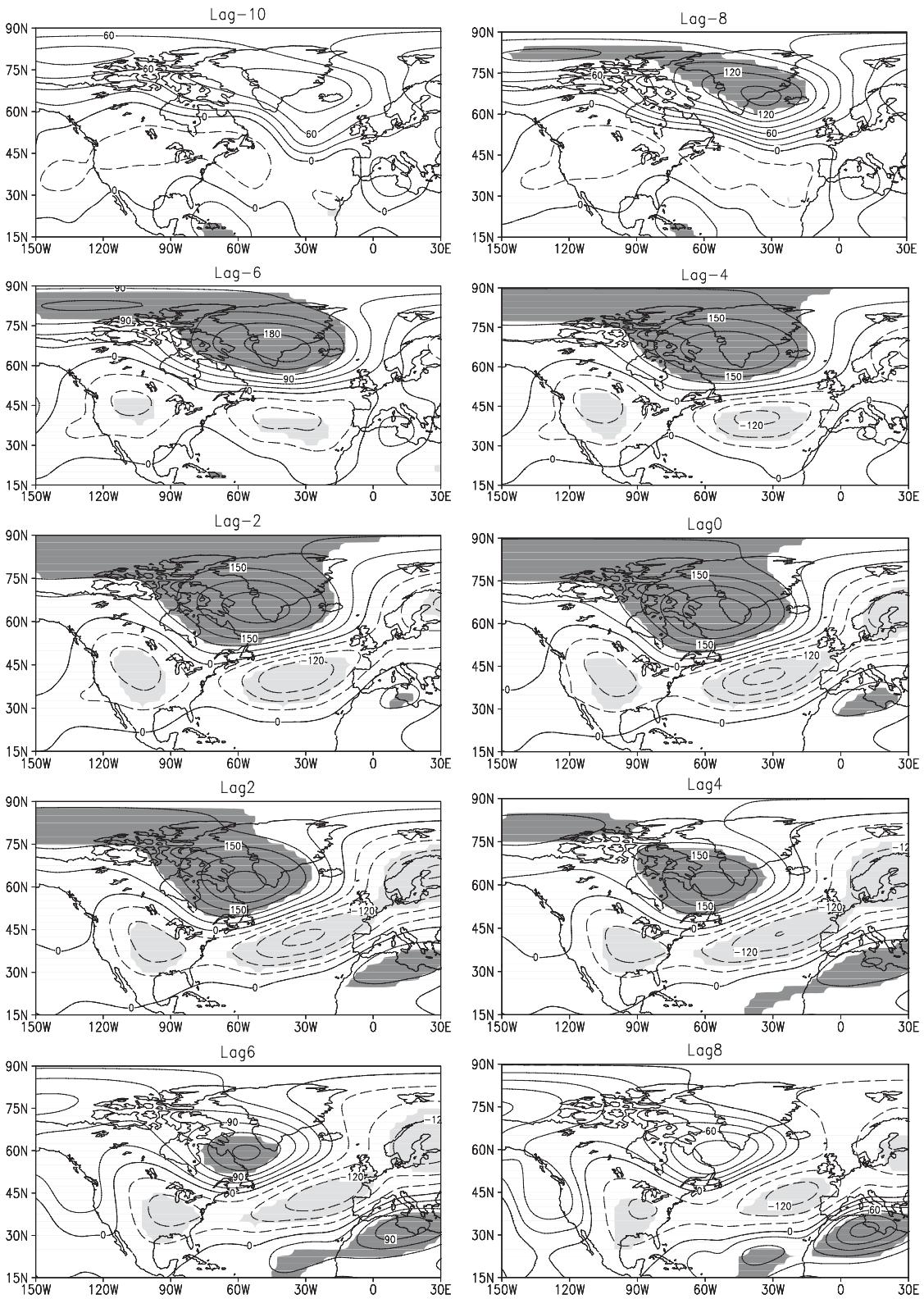
(a)

FIG. 3. As in Fig. 2 but for the period 1978–97 (P2).
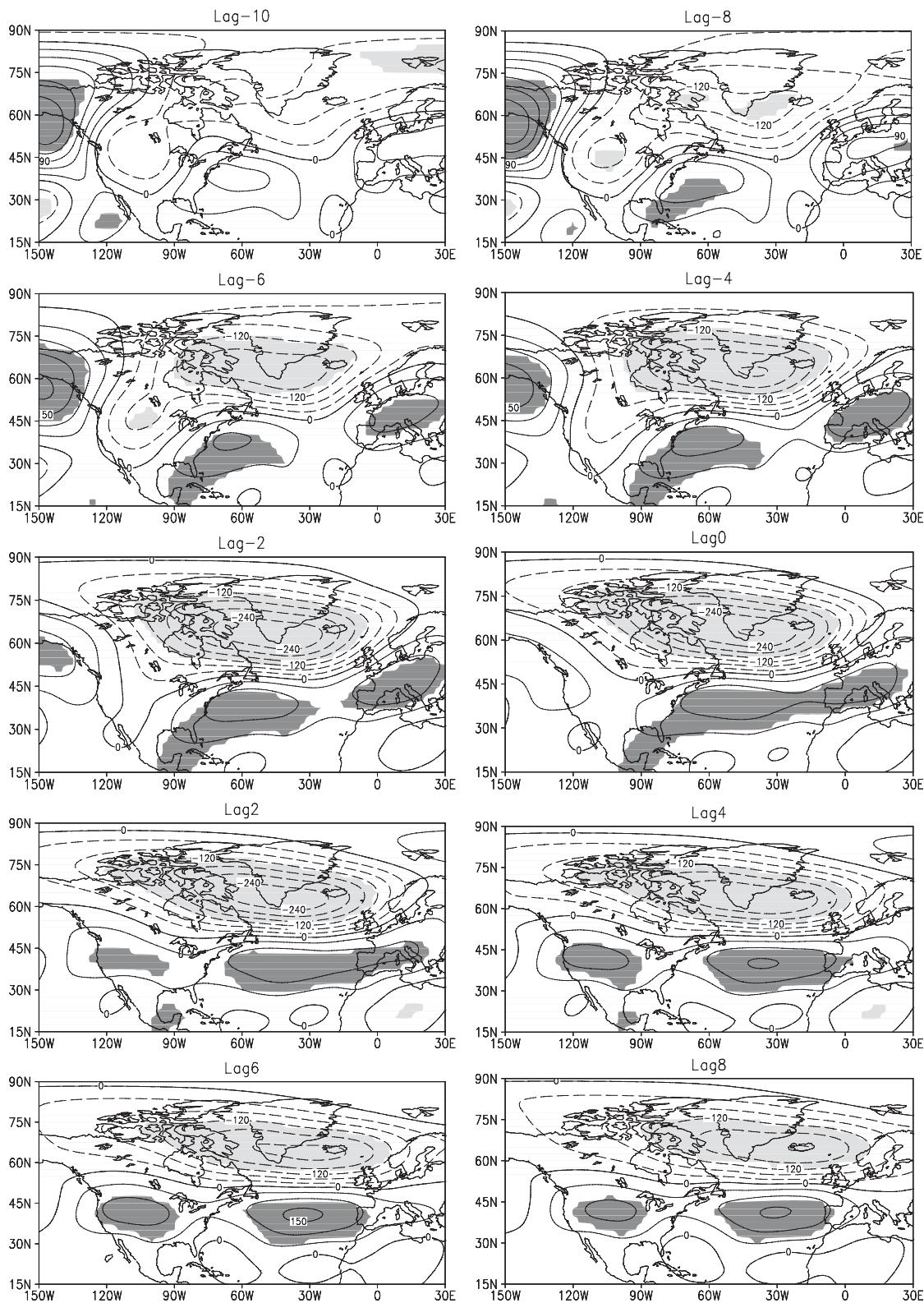
(b)

FIG. 3. (*Continued*)
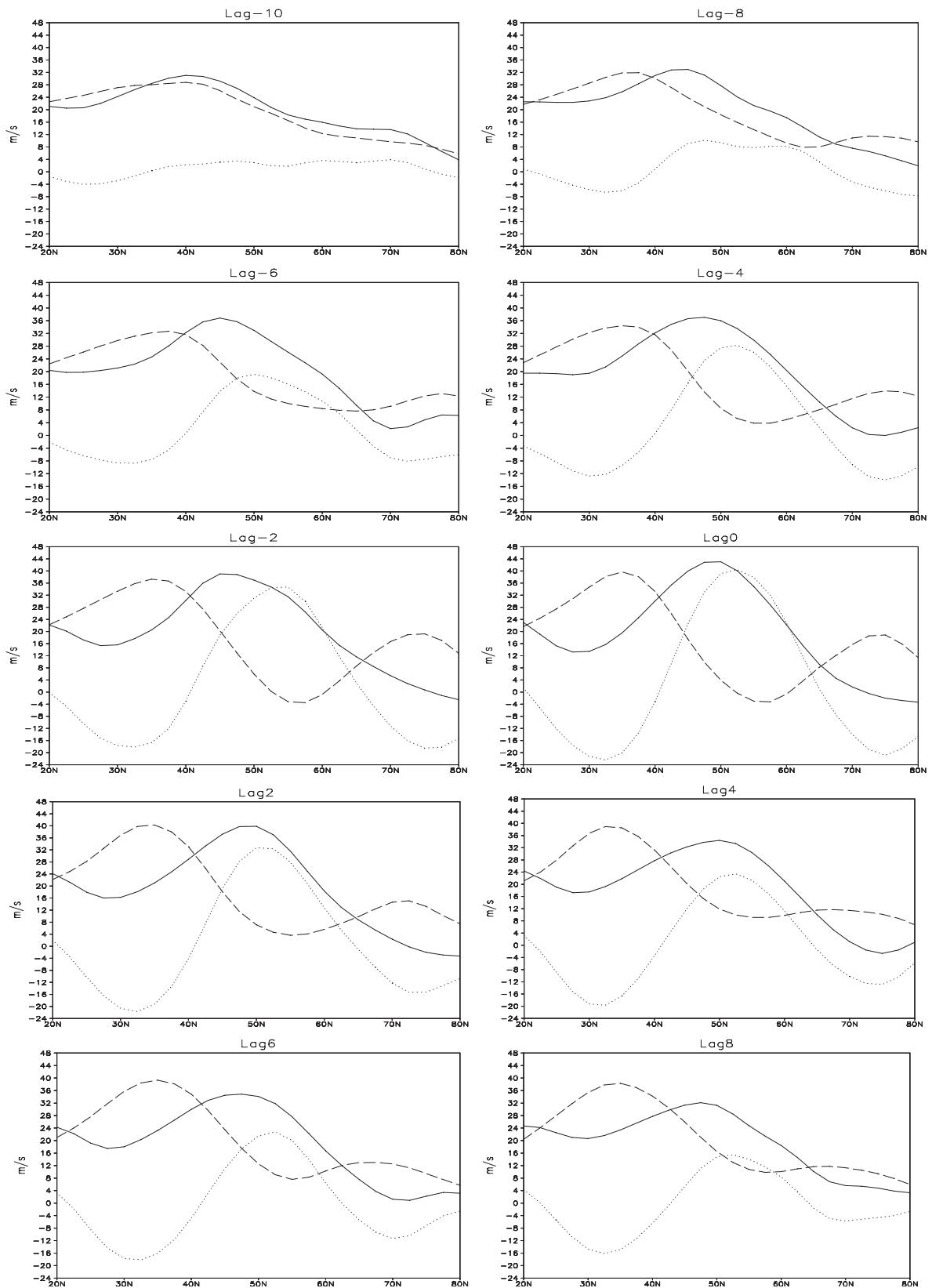
FIG. 4. Composites of the zonal mean zonal winds at 250 mb in the Atlantic sector (90°W–0°) for positive and negative phase NAO events. The solid (dashed) line represents the positive (negative) phase; the dotted line denotes the difference between positive and negative NAO phases.
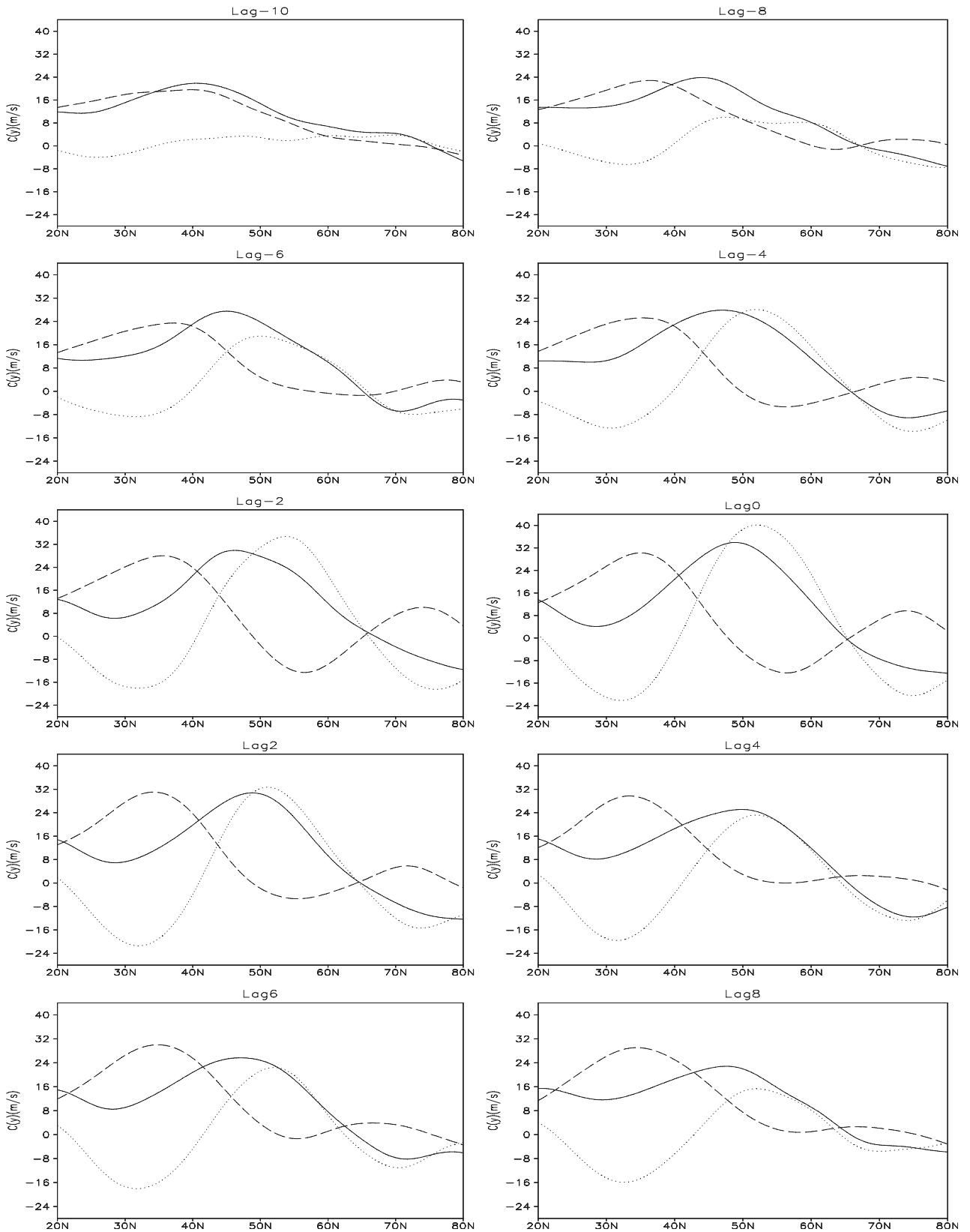
FIG. 5. Zonal phase speed of the linear Rossby wave for the basic flows as shown in Fig. 4. The solid (dashed) line represents the positive (negative) NAO phase; the dotted line denotes the difference of the phase speed between the positive and negative NAO phases.
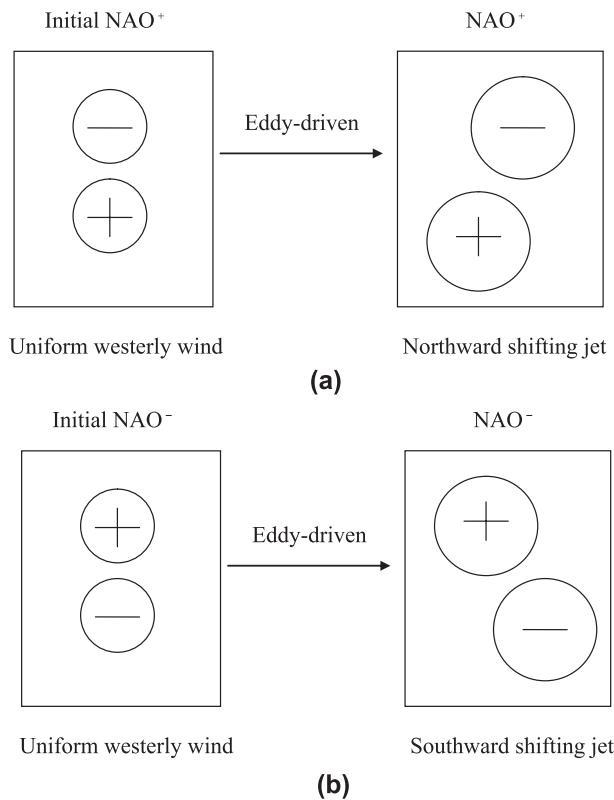
FIG. 6. Idealized schematic of the NAO anomaly for the different phase of the NAO: the (a) positive and (b) negative NAO phases.

dominated by the meridional shift of the Atlantic jet associated with different phases of the NAO event.

Because the difference of the Atlantic jet between the positive and negative NAO phases is more prominent in the higher latitudes than in lower latitudes (Fig. 4), the difference of $C(y)$ between the two phases is larger in the higher than in the lower latitudes. This implies that the eastward shift of the northern center of the NAO pattern is more distinct from the negative to the positive phase, whereas the zonal shift of its southern center is less distinct. In this case, it is inevitable to observe a marked eastward shift of the northern center of the NAO pattern from P1 to P2.

4. Eastward shift of the center of action of the NAO pattern and its possible link with the Atlantic storm-track eddy activity

a. Eastward shift of the Atlantic storm-track eddy activity during P2 and P3

The result described above fails to explain why there is a whole eastward shift of the center of the NAO action although it is able to explain the marked eastward shift of the northern center of the NAO pattern from P1 to P2. Observational studies indicated that the NAO event

and Atlantic storm-track eddy activity are mutually dependent on each other (Hurrell 1995b; Rogers 1997; Jung et al. 2003). Rogers (1997) found a possible link between the increasing baroclinic wave activity over the northeast Atlantic and Europe and a northeastward shift of the NAO anomalies. However, it is still unclear whether the Atlantic storm-track eddy activity is mainly steering the NAO or vice versa, or whether both aspects are inseparably connected.

Here we propose a possible hypothesis that the eastward shift of the Atlantic storm-track eddy activity during P2 is a possible cause of the whole eastward shift of the NAO pattern from P1 to P2. A weakly nonlinear NAO model developed by Luo et al. (2007b) is used to test this hypothesis. Before doing this, we show the spatial distributions of the wintertime mean 2–7-day time scale eddy kinetic energy (EKE) at 250 mb in the Atlantic region in Fig. 7 during P1, P2, and P3. It is seen that the Atlantic storm-track eddy activity undergoes an eastward shift from P1 to P2, which may be associated with the eastward stretch of the Atlantic jet exit region during P2 (not shown). At the same time, it also exhibits a more prominent eastward shift during P3 than during P2. Our calculation also shows that the difference of the Atlantic storm-track eddy activity between P1 and P2/P3 is statistically significant (Figs. 7d–f). Chang and Fu (2002) found that the Pacific and Atlantic storm tracks exhibit a simultaneous strengthening and weakening trend, and there is a transition during the early 1970s from a weak storm track state (prior to 1972/73) to a strong storm track state subsequently. Thus, the variability of the Atlantic storm-track eddy activity from P1 to P2 is probably related to the observed climate shift in the mid-1970s in the Pacific region. However, the study of this issue is beyond the scope of this paper.

Since the Atlantic storm-track eddy activity is located more eastward during P2 than during P1, the preexisting synoptic-scale waves that drive the NAO dipole anomaly should be located more eastward during P2. In this case, the weakly nonlinear analytical solution of Luo et al. (2007b) can probably be used to investigate how the zonal position of the preexisting synoptic-scale waves affects the center of action of the NAO pattern. For this reason, the longitudinal position of the preexisting synoptic-scale eddies may be prescribed to be different in the following discussions.

b. Weakly nonlinear model of NAO events

To test the above hypothesis as a simplest case, a nonlinear barotropic model is used here. As shown in Fig. 4, at lag 10 (where lag 10 is the tenth day prior to the zero-lag day), although the mean westerly wind at 250 mb prior to the NAO onset is larger in the upper troposphere than
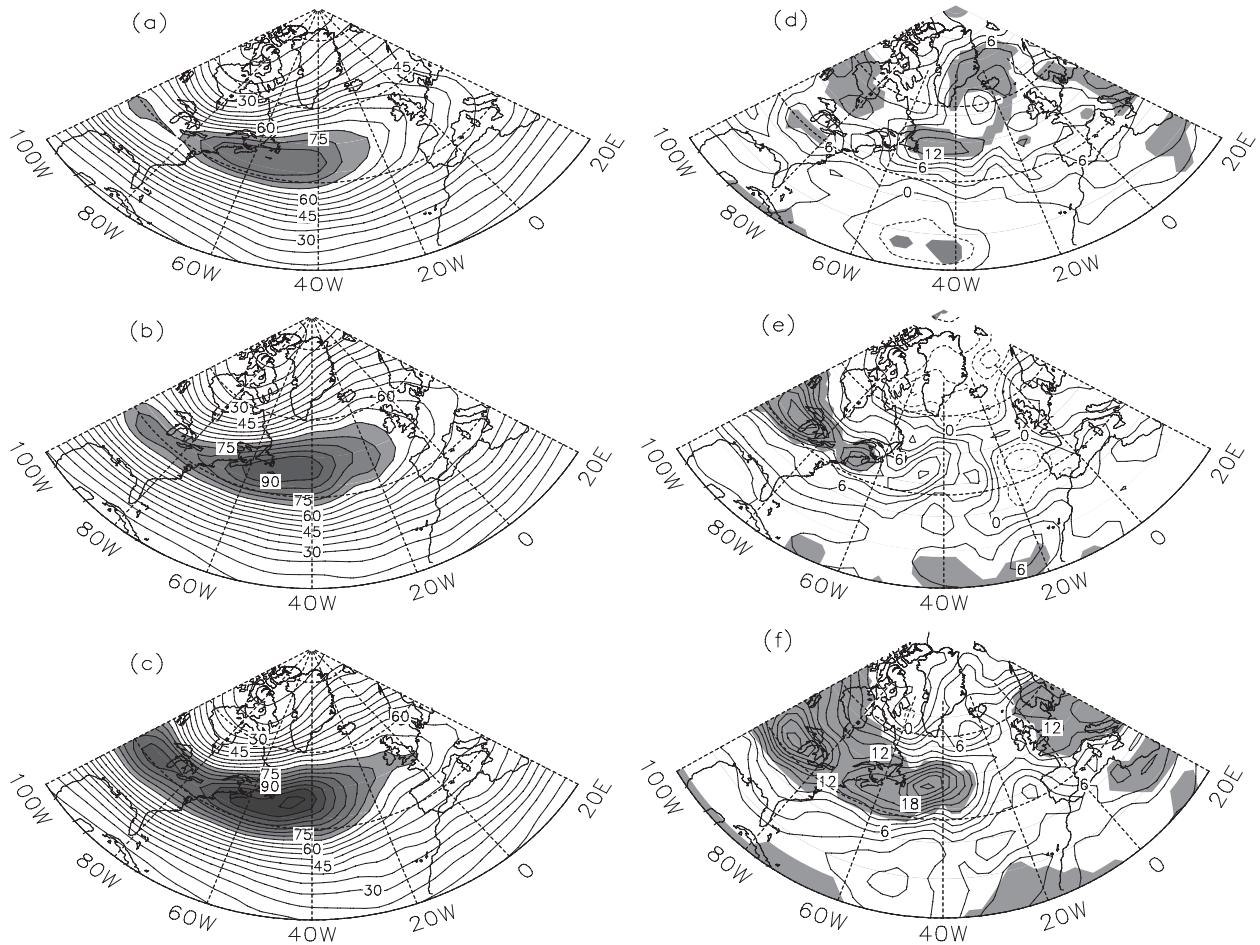
FIG. 7. Winter mean 2–7-day eddy kinetic energy (m² s⁻²) at 250 mb in the Atlantic region for the periods of (a) 1958–77 (P1), 1978–97 (P2) and 1998–2007 (P3) and differences between (d) P2 and P1 (P2 minus P1) (e) P3 and P2 (P3 minus P2), and (f) P3 and P1 (P3 minus P1). The shading in (a)–(c) denotes the region of the EKE greater than 75 m² s⁻², and the shading in (d)–(f) denotes the regions that exceed the 95% confidence level for a Student's *t* test.

in the lower troposphere, the vertical and latitudinal mean of the prior mean westerly winds can be weak because the mean westerly wind is generally weak in the lower troposphere of higher latitudes (not shown). In this case, the vertically and regionally averaged mean westerly wind prior to the NAO onset is supposed to be uniform and relatively weak in that our attention is only focused on the physical mechanism of the eastward shift of the NAO pattern. As a qualitative description of the NAO dynamics this assumption is acceptable. Thus, the weakly nonlinear NAO model developed by Luo et al. (2007b) can be used to test our hypothesis that during P2 the whole eastward shift of the NAO pattern is related to the eastward shift of the Atlantic storm-track eddy activity.

On one hand, the most important assumption of the weakly nonlinear analytical model used here is that there is a clear scale separation between the NAO pattern and transient synoptic-scale waves. This scale separation has

an observational basis. This is because the NAO dipole anomaly/northern annular mode has generally a barotropic vertical structure with zonal wavenumbers 1–2 (Thompson and Wallace 1998), while the NH transient synoptic-scale waves are dominated by zonal wavenumbers 7–18 (Blackmon 1976; White 1980). This can be seen from the numerical result of a two-layer model by Vautard et al. (1988), who found that in a baroclinic jet the atmospheric variability can be separated into a large-scale, quasi-stationary dipole structure with zonal wavenumbers 1–2 and small-scale, high-frequency monopole traveling disturbances with zonal wavenumbers 7–11. In fact, this scale separation assumption can be also verified theoretically (Luo 2005). For example, in a weak uniform basic flow, if a planetary wave with zonal wavenumber 2 is stationary, the zonal wavenumbers of the linear Rossby waves with periods less than one week (synoptic scale) must be greater than 9 (Luo et al. 2007b).

In this case, it is evident that the scale separation assumption used to derive the weakly nonlinear NAO analytical solution is approximately held. Of course, this scale separation assumption may be violated if the synoptic-scale waves are of lower zonal wavenumbers. Even so, it is applicable to the real NAO process because we focus only on the dynamical process of the NAO event (Luo et al. 2007a,b).

On the other hand, another important assumption of the weakly nonlinear NAO analytical model is that in the weakly nonlinear asymptotic solution the first-order term is generally assumed to be larger than the second-order term, but this assumption is easily violated at the strongest stage of the NAO event. Therefore, in the real application the weakly nonlinear asymptotic solution is also thought of as being correct even if the second-order term is the same as, or larger than, the first-order term. Otherwise, no weakly nonlinear theory can be applicable to the observed blocking and NAO phenomena because they are strongly nonlinear. Thus, in the real atmosphere the weakly nonlinear limit is, in general, removed when the weakly nonlinear solutions are applied (Haines and Malanotte-Rizzoli 1991). Because the weakly nonlinear solutions derived by Luo et al. (2007b) can qualitatively capture the main characteristics of observed NAO events, it is at least reasonable to use these solutions to investigate our problems noted above.

For a nondimensional streamfunction Ψ scaled with the characteristic length and velocity corresponding to $L = 1000$ km and $U_0 = 10$ m s^{-1}, if it is divided into three parts—the basic state flow $[\overline{\psi}(y) = -u_0 y$ in which u_0 is a constant], the planetary-scale $[\psi(x, y, t)]$, and synoptic-scale $[\psi'(x, y, t)]$ parts—then the planetary- and synoptic-scale equations can be derived under the scale separation assumption (Luo et al. 2007a,b). Similar to Luo et al. (2007b), the nondimensional equations of the interaction between planetary- and synoptic-scale waves can be expressed as

$$\left(\frac{\partial}{\partial t} + u_0 \frac{\partial}{\partial x}\right)(\nabla^2 \psi - F\psi) + J(\psi, \nabla^2 \psi + h)$$
$$+ (\beta + Fu_0)\frac{\partial \psi}{\partial x} + u_0 \frac{\partial h}{\partial x} = -J(\psi', \nabla^2 \psi')_P, \quad (3a)$$

and

$$\left(\frac{\partial}{\partial t} + u_0 \frac{\partial}{\partial x}\right)(\nabla^2 \psi' - F\psi') + (\beta + Fu_0)\frac{\partial \psi'}{\partial x}$$
$$= -J(\psi', \nabla^2 \psi + h) - J(\psi, \nabla^2 \psi') + \nabla^2 \psi_S^*, \quad (3b)$$

where ψ and ψ' are the planetary-scale and synoptic-scale streamfunction anomalies respectively; $F = (L/R_d)^2$, where R_d is the radius of Rossby deformation; and $\beta = \beta_0 L^2/U_0$

is the nondimensional meridional gradient of the Coriolis parameter centered at ϕ_0. In Eq. (3b) $\nabla^2 \psi_S^*$ is the synoptic-scale vorticity source introduced to maintain synoptic-scale waves upstream of the NAO region, but $-J(\psi', \nabla^2 \psi')_P$ in Eq. (3a) is a planetary-scale part of the eddy vorticity flux induced by synoptic-scale eddies and is referred to as the "eddy vorticity forcing" hereafter. The other notation can be found in Luo et al. (2007b).

In the NH the large-scale topography in the mid to high latitudes is generally approximated as two continents and two oceans, a wavenumber-2 topography (Charney and DeVore 1979). In this case, if one assumes $h = \varepsilon h'$, h' can be assumed to be of the form of $h' = h_0' \exp[ik(x + x_T)]\sin(my/2)$ + c.c. in which h_0' is the amplitude of the wavy topography with the zonal wavenumber $k = 2/[6.371\cos(\phi_0)]$ at a given latitude ϕ_0, x_T is the position of the dipole mode such as the NAO anomaly relative to the topographic trough, and $m = \pm 2\pi/L_y$. It should be pointed out that $h_0' > 0$ represents a topographic trough in the North Atlantic sector for $m = -2\pi/L_y$, but $h_0' < 0$ does so for $m = 2\pi/L_y$. Here we assume $u_0 = \beta/(k^2 + m^2) \approx 0.7$ ($\omega \approx 0$) to allow the dipole mode to be quasi stationary before the life cycle of a NAO event begins.

To obtain the weakly nonlinear asymptotic solution of the nonlinear barotropic vorticity equation, some assumptions must be made as in Luo et al. (2007b). The most important point of this assumption is that the phase speed of the leading-order Rossby wave does not include the change of the mean flow induced by the feedbacks of the NAO anomaly and the topographic wave because the variation of the mean flow induced by the NAO anomaly is considered as the second-order solution. Thus, the weakly nonlinear analytical solution derived by Luo et al. (2007b) cannot represent the northeast–southwest or northwest–southeast tilting of the NAO pattern. However, it can be applied to our problem because our emphasis is on the cause of the whole eastward shift of the center of action of the NAO pattern. For this reason, it is useful to review the planetary- and synoptic-scale analytical solutions of the NAO life cycle derived by Luo et al. (2007b). In a fast-variable form the weakly nonlinear analytical solutions of the life cycle of the eddy-driven NAO event can be written as

$$\psi_P = -u_0 y + \psi \approx -u_0 y + \psi_{NAO} + \psi_C + \psi_M, \quad (4a)$$

$$\psi_{NAO} = B(x, t)\sqrt{\frac{2}{L_y}}\exp(ikx)\sin(my) + \text{c.c.}, \quad (4b)$$

$$\psi_C = h_A h_0 \exp[ik(x + x_T)]\sin\left(\frac{m}{2}y\right) + \text{c.c.}, \quad (4c)$$

$$\psi_M = \psi_{m1} + \psi_{m2}, \quad (4d)$$

$$\psi_{m1} = -|B|^2 \sum_{n=1}^{\infty} q_n g_n \cos(n+1/2)my, \quad (4e)$$

$$\psi_{m2} = -h_0 h_A \sqrt{\frac{2}{L_y}} (Be^{-ikx_T} + B^* e^{ikx_T})$$

$$\times \sum_{n=1}^{\infty} \tilde{q}_n (3a_n - b_n) \cos(nmy), \quad (4f)$$

$$\psi' \approx \varepsilon^{3/2} (\tilde{\psi}'_0 + \varepsilon \tilde{\psi}'_1) = \psi'_1 + \psi'_2, \quad (4g)$$

$$\psi'_1 = f_0(x)\{\exp[i(\tilde{k}_1 x - \tilde{\omega}_1 t)]$$

$$+ \alpha \exp[i(\tilde{k}_2 x - \tilde{\omega}_2 t)]\} \sin\left(\frac{m}{2}y\right) + \text{c.c.}, \quad (4h)$$

$$\psi'_2 = \psi'_{NAO} + \psi'_T, \quad (4i)$$

$$\psi'_{NAO} = -\frac{m}{4}\sqrt{\frac{2}{L_y}} Q_1 B f_0 \exp\{i[(\tilde{k}_1 + k)x - \tilde{\omega}_1 t]\}\left[p_1 \sin\left(\frac{3m}{2}y\right) + r_1 \sin\left(\frac{m}{2}y\right)\right]$$

$$- \alpha \frac{m}{4}\sqrt{\frac{2}{L_y}} Q_2 B f_0 \exp\{i[(\tilde{k}_2 + k)x - \tilde{\omega}_2 t]\}\left[p_2 \sin\left(\frac{3m}{2}y\right) + r_2 \sin\left(\frac{m}{2}y\right)\right]$$

$$+ \frac{m}{4}\sqrt{\frac{2}{L_y}} Q_1 B^* f_0 \exp\{i[(\tilde{k}_1 - k)x - \tilde{\omega}_1 t]\}\left[s_1 \sin\left(\frac{3m}{2}y\right) + h_1 \sin\left(\frac{m}{2}y\right)\right]$$

$$+ \alpha \frac{m}{4}\sqrt{\frac{2}{L_y}} Q_2 B^* f_0 \exp\{i[(\tilde{k}_2 - k)x - \tilde{\omega}_2 t]\}\left[s_2 \sin\left(\frac{3m}{2}y\right) + h_2 \sin\left(\frac{m}{2}y\right)\right] + \text{c.c.}, \quad (4j)$$

and

$$\psi'_T = -\frac{m}{4} f_0 h_0 \pi_1 \exp\{i[(\tilde{k}_1 + k)x + kx_T - \tilde{\omega}_1 t]\} \sin(my) - \alpha \frac{m}{4} f_0 h_0 \pi_2 \exp\{i[(\tilde{k}_2 + k)x + kx_T - \tilde{\omega}_2 t]\} \sin(my)$$

$$- \frac{m}{4} f_0 h_0 \sigma_1 \exp\{i[(\tilde{k}_1 - k)x - kx_T - \tilde{\omega}_1 t]\} \sin(my) - \alpha \frac{m}{4} f_0 h_0 \sigma_2 \exp\{i[(\tilde{k}_2 - k)x - kx_T - \tilde{\omega}_2 t]\} \sin(my) + \text{c.c.},$$

$$(4k)$$

where $\alpha = \pm 1$, $m = \pm 2\pi/L_y$, $h_A = -1/[\beta/u_0 - (k^2 + m^2/4)]$, $h_0 = \varepsilon h'_0$,

$$a_n = \frac{6}{m[(3/2)^2 - n^2]L_y}, \quad b_n = \frac{2}{m[(1/2)^2 - n^2]L_y},$$

$$\tilde{q}_n = \frac{k^2 m}{2\{\beta + Fu_0 - (u_0 - C_g)[(nm)^2 + F]\}},$$

and $f_0(x) = a_0 \exp[-\mu\varepsilon^2(x + x_0)^2]$ denotes the zonal distribution of the eddy amplitude, in which a_0 denotes the intensity of the storm-track eddies, $\mu > 0$, $x = -x_0$ represents the position of the upstream storm track eddies relative to the initial NAO anomaly center, $\varepsilon > 0$ is a small parameter, B^* is the complex conjugate of B, and the other coefficients and notation can be found in Luo et al. (2007b). Changing x_0 can represent the different position of the eddy activity, but the magnitude of μ may reflect the zonal localization (width) of the eddy activity. When x_0 is chosen to be smaller, it can represent the eastward shift of the Atlantic storm-track eddy activity. In deriving Eq. (4), $\nabla^2 \psi_s^*$ has been assumed to balance the preexisting synoptic-scale eddies upstream given in Eq. (4h). But

the traveling eddy forcing with its amplitude of slow time scales that arises from the synoptic-scale wave packets upstream is not included in our present theoretical model.

With a weakly nonlinear asymptotic method it is easy to get the amplitude equation of the eddy-driven NAO anomaly under the forcings of both the storm track eddies and large-scale topography. This amplitude equation is the so-called forced nonlinear Schrödinger (NLS) equation (Luo et al. 2007b), which is of the form of

$$i\left(\frac{\partial B}{\partial t} + C_g \frac{\partial B}{\partial x}\right) + \lambda \frac{\partial^2 B}{\partial x^2} + \delta|B|^2 B + \tilde{\alpha}h_0^2(B + B^* e^{i2kx_T})$$

$$+ Gf_0^2 \exp[-i(\Delta kx + \Delta\omega t)] = 0, \quad (5)$$

where

$$\tilde{\alpha} = -\frac{kmh_A}{4(k^2 + m^2 + F)} \sum_{n=1}^{\infty} \tilde{q}_n (3a_n - b_n)^2$$

$$\times \{[(nm)^2 - (k^2 + m^2/4)]h_A + 1\},$$

$k - (\tilde{k}_2 - \tilde{k}_1) = \Delta k$, and $\tilde{\omega}_2 - \tilde{\omega}_1 - \omega = \Delta\omega$ ($\omega \approx 0$); the other coefficients can be found in Luo et al. (2007b).

In Eq. (4b), ψ_{NAO} represents the eddy-driven NAO dipole anomaly. When the solution $B(x, t)$ is obtained

for a given initial value, the temporal and spatial evolution of the NAO dipole anomaly ψ_{NAO} can be known. Although ψ in Eq. (3a) or (4a) is a planetary-scale anomaly, it actually contains the time variation part of the basic flow due to the feedback of the planetary-scale anomaly. This is because $\psi(x, y, t)$ can be divided into three parts: ψ_M, ψ_{NAO}, and ψ_C. Here ψ_{NAO} is the NAO anomaly and ψ_C is the stationary wave anomaly induced by the topography; $\psi_M = \varepsilon^2 \overline{\psi}_2(\varepsilon x, \varepsilon^2 x, \varepsilon t, \varepsilon^2 t, y)$, and $\overline{\psi}_2$ is the spatially and temporally slow variation of the basic flow induced by the feedback of the planetary-scale anomalies that is the second-order approximation of our asymptotic solution (Luo et al. 2007a,b), but ψ_{NAO} and ψ_C are the first-order approximations. It is evident that the time-dependent mean westerly wind during the NAO life cycle can be obtained as $U = u_0 + u_{NAO}$ from Eq. (4d), where $u_{NAO} = -\partial \psi_M / \partial y$ is the westerly jet anomaly. On the other hand, since u_{NAO} includes the amplitude B of the NAO anomaly, changes in the westerly jet and NAO anomalies are dependent on each other. There is also $U \approx u_0$ at the beginning of the NAO event because the NAO amplitude B is rather small at that time. But when the NAO anomaly is large, the change in the westerly jet anomaly is large. Thus, as indicated by Luo et al. (2007b), the changes in the westerly jet and NAO anomalies are the same entity, being only different descriptions of the same phenomenon. Once the interaction between planetary- and synoptic-scale waves occurs, the westerly jet and NAO anomalies are coupled together. An efficient method of treating our problem is that the westerly jet anomaly arising from the feedback of the eddy-driven NAO anomaly is considered as the second-order approximation of the NAO anomaly (Luo et al. 2007a,b). Although this assumption is not exact for the variation of the observed Atlantic jet during the NAO life cycle, it can allow us to analytically treat the interaction among the mean flow and planetary- and synoptic-scale waves. Moreover, the time evolution of the westerly jet anomaly obtained from our theoretical solutions is found to be qualitatively consistent with the observations (Luo et al. 2007b).

Equation (4h) is the synoptic-scale wave prior to the NAO onset, while Eqs. (4j) and (4k) are the synoptic-scale wave components induced by the feedback of the NAO dipole anomaly and a topographic wave respectively. Here both $\alpha = -1$ and $m = -2\pi/L_y$ represent the negative phase of the NAO, whereas $\alpha = 1$ and $m = 2\pi/L_y$ correspond to the positive phase. In our previous papers the analytical solutions have been successfully used to describe the main characteristics of observed NAO events (Luo et al. 2007a,b). Here, they are only used to interpret the whole eastward shift of the NAO pattern.

In an unfiltered field of an observed NAO event the occurrence of the NAO event looks like the remnant of breaking waves (Benedict et al. 2004; Franzke et al. 2004). This seems to be at odds with the scale separation assumption. In fact, the wave breaking seen in the unfiltered field of an observed NAO event is not inconsistent with the scale separation assumption used in our theoretical model. This is because the unfiltered field actually comprises the basic flow (zonal wavenumber zero), the NAO anomaly (planetary-scale part), and synoptic-scale eddies although they are dependent on each other during their interaction. As demonstrated by Luo et al. (2007a,b), the feedback of the amplified NAO anomaly on synoptic-scale waves can cause the breaking of synoptic-scale waves. The process of synoptic-scale wave breaking is easily understood in terms of the analytical solution Eq. (4). As described in Eq. (4), the total field of a NAO event is $\Psi = \overline{\psi}(y) + \psi_M + \psi_{NAO} + \psi_C + \psi'$ (where $\overline{\psi} = -u_0 y$), which corresponds in fact to the unfiltered field of the observed NAO event. Before the interaction between planetary and synoptic scales occurs, the planetary-scale (k) and synoptic-scale ($\tilde{k}_i$, $i = 1, 2$) waves are independent of each other. For this case, as a mechanism study it is at least reasonable to suppose that prior to the NAO occurrence there is a scale separation ($\tilde{k}_i \gg k$) between the planetary- and synoptic-scale waves. Once the NAO anomaly is amplified by preexisting synoptic-scale waves with zonal wavenumber $\tilde{k}_i$, the amplified NAO anomaly ψ_{NAO} can exert a feedback onto the preexisting synoptic-scale waves. In this case, subsequent synoptic-scale waves will inevitably include the effect of the NAO anomaly with zonal wavenumber k and will comprise wavenumber components $\tilde{k}_i$ and $\tilde{k}_i \pm k$. Thus, during the life cycle of a NAO event the NAO anomaly and synoptic-scale waves can be coupled together. Since the NAO anomaly and preexisting synoptic-scale waves are assumed to be zonally separated, there is $\tilde{k}_i \pm k \approx \tilde{k}_i$ due to $k \ll \tilde{k}_i$. In this case, wavenumber components $\tilde{k}_i \pm k$ of ψ' are still within a synoptic-scale range. Thus, the scale separation between the NAO anomaly ψ_{NAO} with zonal wavenumber k and deformed synoptic-scale eddies ψ' with zonal wavenumbers $\tilde{k}_i \pm k$ still holds during the NAO life cycle even though the breaking of synoptic-scale waves can occur. It should be pointed out that, although the NAO anomaly ψ_{NAO} comprises the envelope amplitude B and its wavenumber k, the zonal scale of the envelope amplitude B is found to be much larger than that of the carrier wave of the NAO anomaly ψ_{NAO}. Thus, there is a scale separation between the envelope amplitude and carrier wave of the NAO anomaly. Since ψ_M includes the envelope amplitude for B, it is natural that there is a scale separation between ψ_M and ψ_{NAO}. In this case, the scale separation between the

TABLE 1. List of prescribed parameters in the weakly nonlinear NAO model.

Parameters	Value
Topographic height h_0	−0.5
Position of positive topographic wave anomaly x_T	−2.0
Wavenumbers of synoptic-scale eddies $\tilde{k}_i$ ($i = 1, 2$)	As in Luo et al. (2007a)
Eddy strength a_0	0.17
Zonal distribution of synoptic-scale eddies μ	2.4
Position of the maximum eddy strength x_0	0~4.0
Positive small parameter ε	0.24
Width of β-plane channel L_y	5.0
Referenced latitude ϕ_0	55°N
Square of the ratio of the length scale and deformation radius F	1.0

FIG. 8. Horizontal distribution of the initial synoptic-scale waves ψ_1' for different x_0, where the longitudinal (latitudinal) coordinate denotes the x (y) direction: (a) $x_0 = 2.87$; (b) $x_0 = 2.87/2$. The contour interval is 0.05.

NAO anomaly and the jet stream anomaly $u_{\text{NAO}} = -\partial \psi_M / \partial y$ is held. On the other hand, because $\overline{\psi} = -u_0 y$ is a zonal mean quantity, there is also a scale separation between the prespecified mean flow $\overline{\psi}(y)$ and the jet stream anomaly u_{NAO}. In conclusion, the scale separation assumption about synoptic-scale waves, the NAO anomaly, and the jet stream anomaly used in our analytical model is valid—at least for the NAO dynamics.

When the NAO anomaly is amplified by preexisting synoptic-scale waves and is strong enough, the breaking of synoptic-scale waves is inevitable. This leads to violation of the weakly nonlinear limit used in our theoretical model because the strongly nonlinear process may be dominant in the wave breaking process. However, the weakly nonlinear solutions are still reasonable in describing the basic characteristics of the NAO event as an approximation of the strongly nonlinear system. This will be verified by the numerical solutions presented in Part II by removing the scale separation and weakly nonlinear assumptions. Thus, it is reasonable to explain why the NAO pattern can undergo an eastward shift by using the weakly nonlinear NAO analytical solutions of Luo et al. (2007b).

Since our interest is aimed at the eastward shift of the NAO pattern, we only present the instantaneous planetary-scale anomaly field ψ_{NAO} of the NAO event in the next subsection.

c. Theoretical results

To examine how the position of the Atlantic storm-track eddy activity affects the zonal shift of the NAO pattern, we can vary x_0 to represent the different position of the synoptic-scale eddy activity relative to the initial NAO anomaly but fix other parameters in our theoretical

model. Here only the positive phase NAO event is considered as an example.

Since the NAO is a nonlinear complex phenomenon related to an interaction between planetary and synoptic scales, its behavior is related to many parameters concerning the basic flow and planetary- and synoptic-scale waves. Although the details of the NAO event obtained from this theoretical model depend slightly on the parameters, its basic characteristics are consistent with the observations (Luo et al. 2007a). The parameters used in this paper are listed in Table 1; they are also the same as those in Luo et al. (2007a,b).

The streamfunction anomalies (ψ_1') of the preexisting synoptic-scale waves at day 0 ($t = 0$) are shown in Fig. 8 for $x_0 = 2.87$ and $x_0 = 2.87/2$. It is evident that Fig. 8a can crudely represent the Atlantic storm-track eddy activity observed during P1 (Fig. 7a), while Fig. 8b is an approximation of the Atlantic storm-track eddy activity during P2 (Fig. 7b). To more clearly see the impact of the different position of preexisting synoptic-scale eddies on the zonal displacement of the NAO anomaly center, and without loss of the generality, we consider $B(x, 0) = 0.4$ as an initial value of the positive phase NAO anomaly. We plot the time evolution of the NAO anomaly during its life cycle for understanding how the position of the NAO anomaly center depends on the different stages of the NAO event. For the parameters shown in Table 1, the
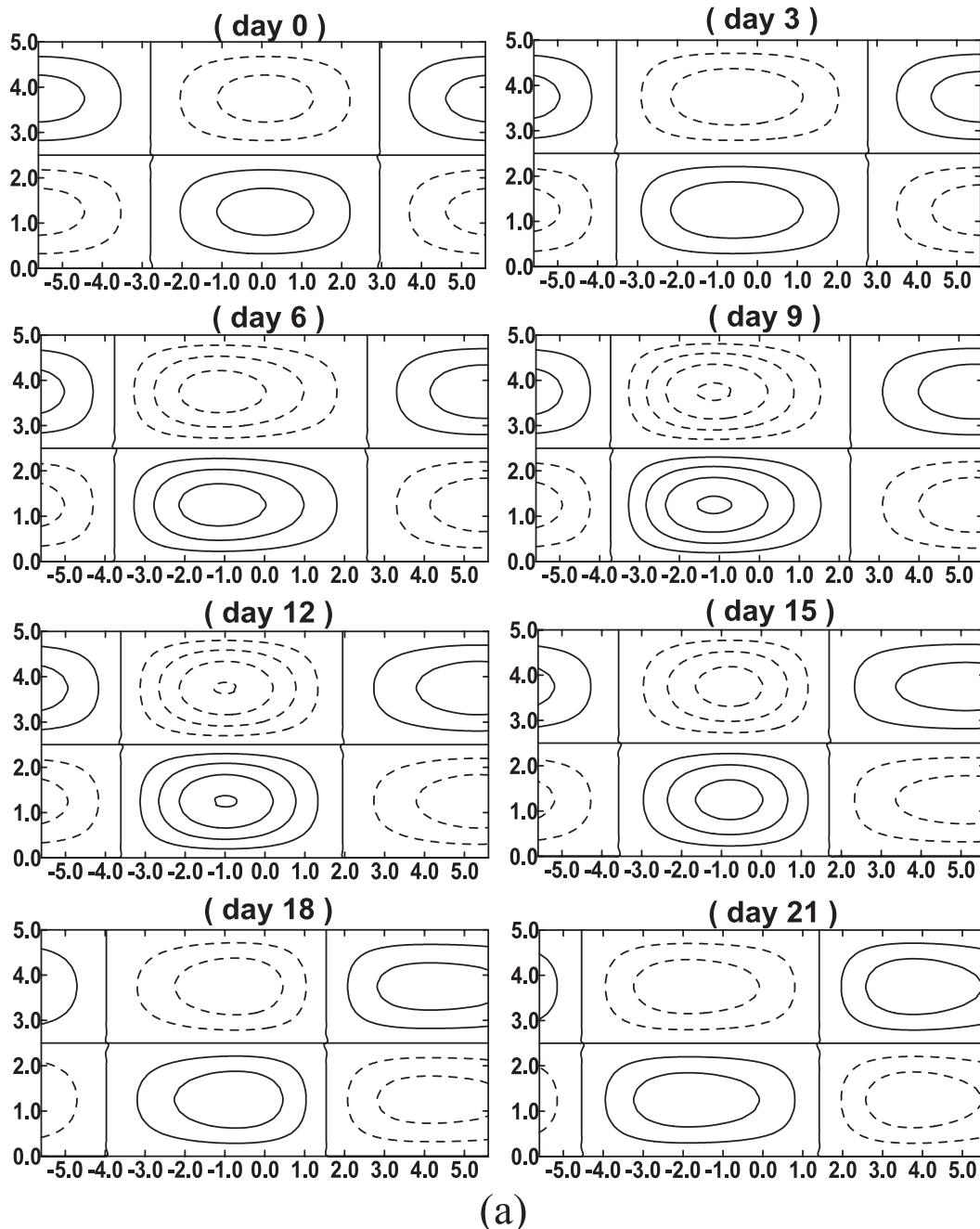
FIG. 9. Time sequences of the eddy-driven positive phase NAO dipole anomaly ψ_{NAO} for different x_0, where the longitudinal (latitudinal) coordinate is in the x (y) direction: (a) $x_0 = 2.87$ and (b) $x_0 = 2.87/2$. The contour interval is 0.2.

time sequences of the life cycle of the eddy-driven positive phase NAO anomaly ψ_{NAO} are shown in Figs. 9a and 9b for $x_0 = 2.87$ and $x_0 = 2.87/2$, respectively.

It is interesting to see that during the positive phase NAO life cycle the eddy-driven NAO dipole anomaly is displaced more westward for $x_0 = 2.87$ than for $x_0 = 2.87/2$, which is particularly evident at the mature stage of the NAO (Fig. 9 at day 9). This indicates that the eddy-driven

NAO pattern would have an eastward shift as the Atlantic storm-track eddy activity exhibits an eastward shift. Of course, the effect of the widening of the region of the synoptic eddy activity on the position of the NAO center is less evident (not shown). Thus, the whole eastward shift of the NAO pattern is more likely to be dominated by the eastward displacement of the storm-track eddy activity in the Atlantic basin. However, the

(b)
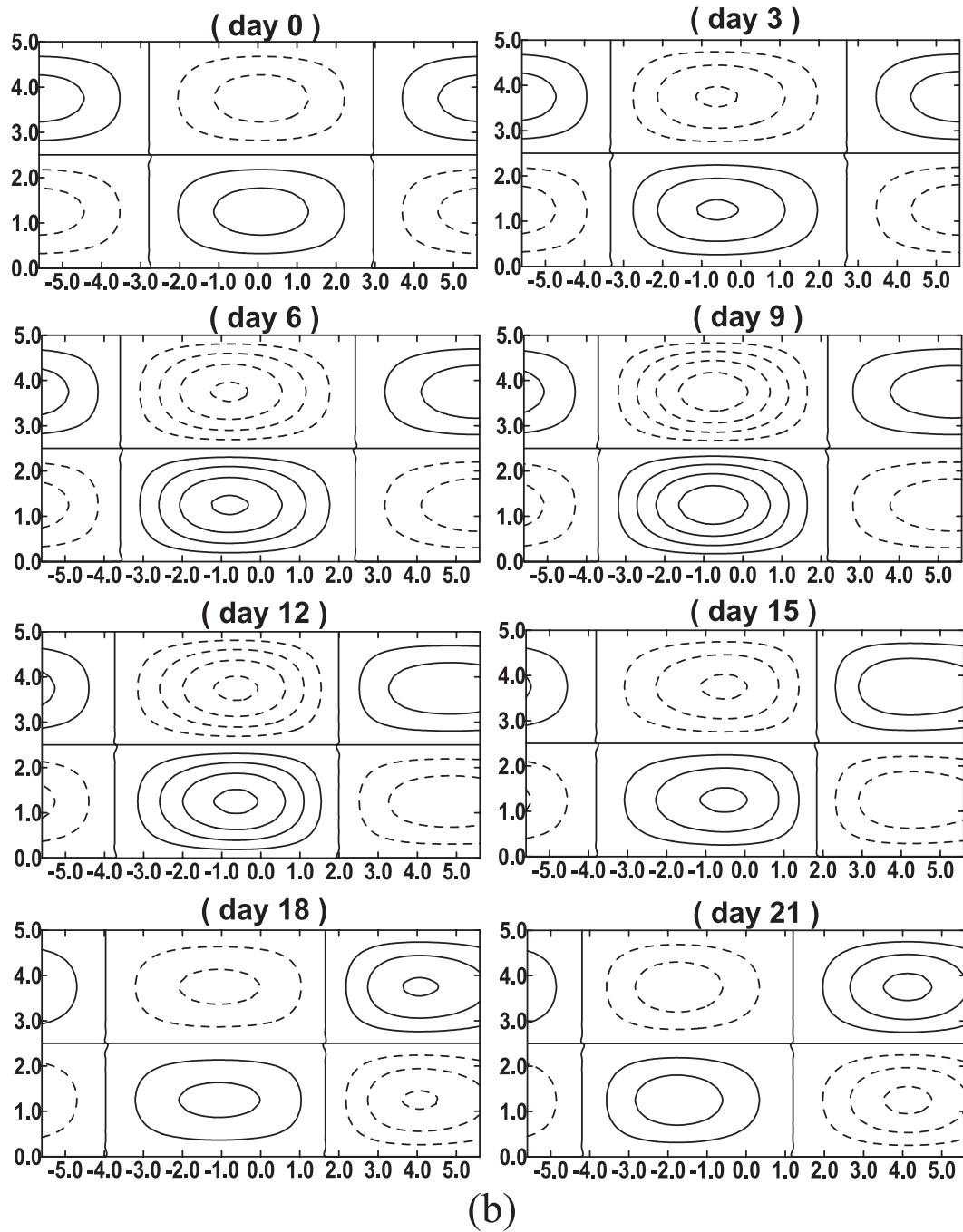
FIG. 9. (*Continued*)

tilting features of the NAO dipole anomaly are not found in our weakly nonlinear analytical solution since the change in the mean flow during the NAO life cycle has been assumed to be the second-order modification of the prespecified background flow. This will naturally exclude the dependence of the propagation speed of the eddy-driven NAO anomaly on the meridional variation

of the mean flow during the NAO life cycle. This is why the eddy-driven NAO dipole, as shown in Fig. 9, does not exhibit a spatial tilting. However, this problem can be solved by the numerical solution performed in Part II of this paper.

Since ψ_{NAO} at day 9 can crudely represent the mature NAO anomaly, the westward displacement distance of
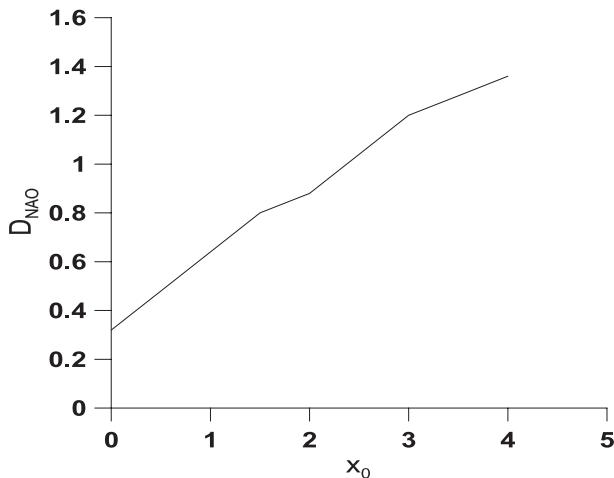
FIG. 10. Westward movement distance D_{NAO} of the eddy-driven NAO dipole anomaly with the position x_0 of the maximum storm-track eddy activity in the Atlantic region.

the NAO anomaly from day 0 to day 9 can be used to describe the zonal position of the eddy-driven NAO anomaly. Here, we define $D_{NAO} = -(x_{NAO} - x_I)$ as the westward movement distance of the eddy-driven NAO dipole pattern at the mature stage relative to its initial position, where x_{NAO} is the position of the NAO anomaly at day 9 from its initial position $x_I = 0$ at day 0. The westward movement distance D_{NAO} of the eddy-driven positive phase NAO pattern is shown in Fig. 10 for different x_0 (the different position of the maximum storm-track eddy activity).

It is seen in Fig. 10 that the center of the eddy-driven NAO anomaly can be understood as being dominated by the longitudinal position of the storm-track eddy activity. When the storm-track eddy activity upstream is located more westward, the westward movement of the eddy-induced NAO dipole is more prominent, and vice versa. In other words, the center of action of the eddy-driven NAO pattern is located more eastward as the Atlantic storm-track eddy activity undergoes an eastward shift. Of course, this result is also held for other parameters, even for weak topography or in the absence of topography (not shown). Thus, the whole eastward shift of the center of action of the NAO pattern during P2/P3 may be closely related to the eastward displacement of the Atlantic storm-track eddy activity. However, it must be pointed out that the NAO pattern for each event can organize the Atlantic storm track and determine its subsequent zonal position because both the NAO pattern and synoptic-scale eddies are strongly coupled (Luo et al. 2007a). Nevertheless, the climatological position of the center of action of the NAO pattern is still dominated by the climatological position of the Atlantic storm-track eddy activity.

Although the result shown in Fig. 9 can, to some extent, explain the whole eastward displacement of the NAO pattern induced by the eastward shift of the Atlantic storm-track eddy activity during P2 and P3, it fails to interpret the nonlinear dependence of the spatial pattern of the NAO on the NAO index noted by Peterson et al. (2003). This is because the phase speed of the eddy-driven NAO dipole anomaly has been assumed to be independent of the change in the mean flow during the NAO life cycle in our highly simplified theoretical model. This is an unresolved and difficult problem in a weakly nonlinear framework, which can be solved by using a numerical solution of a fully nonlinear barotropic vorticity equation, presented in Part II. Nevertheless, our theoretical result is still useful for understanding the main cause of the eastward shift of the center of action of the NAO pattern during P2 and P3. It is thus concluded that the whole eastward shift of the eddy-driven NAO anomaly during P2 and P3 is attributable to the eastward shift of the Atlantic storm-track eddy activity. Ulbrich and Christoph (1999) found in a coupled ECHAM4 /OPYC3 model that increasing greenhouse gas concentrations are a main cause of the whole eastward shift of the NAO pattern. This argument is easily understood according to our results. Increasing greenhouse gas forcing can generally enhance the mean flow in the mid to high latitudes (Sigmond et al. 2004) and finally cause the eastward displacement of the enhanced storm-track eddy activity. As a result, the eastward displacement of the Atlantic storm-track eddy activity can induce the eastward shift of the NAO pattern.

5. Conclusions and discussion

In this paper, we have investigated the physical causes for why the NAO pattern undergoes an eastward shift from the period 1958–77 (P1) to the period 1978–97 (P2) or 1998–2007 (P3) from observational and theoretical aspects. It is found that 1) the northward shift of the jet stream core from the south to the north as the NAO transits from the negative to the positive phases and 2) the eastward shift of the Atlantic storm-track eddy activity associated with the increase of the mean flow in the eastern Atlantic region are the two main causes of the eastward shift of the center of action of the NAO during P2 (P3). The NE–SW (NW–SE) tilting of the NAO pattern is a natural outcome of the occurrence of the positive (negative) phase of the NAO. During the period of the positive (negative) NAO phase, the Atlantic jet stream is inevitably shifted to the north (south) due to the feedback of the NAO dipole anomaly and its interaction with a topographic wave. As a result, the eastward movement of the positive (negative) NAO phase dipole anomaly is faster (slower) in the higher latitudes

than lower latitudes according to the phase speed formula of a linear Rossby wave in a slowly varying media for a basic flow with latitudinal shear. This process tends to cause either the northeast–southwest or northwest–southeast tilting of the NAO dipole anomaly, depending on the phase of the NAO. On the other hand, the eastward shift of the northern center of the NAO seems more prominent because the difference of the mean flow between the two phases of the NAO is more distinct in higher latitudes than in lower latitudes.

In addition, observations show that the wintertime Atlantic storm-track eddy activity exhibits a pronounced eastward displacement from P1 to P2/P3. A weakly nonlinear analytical solution by Luo et al. (2007b) is used to confirm that the eastward shift of the Atlantic storm-track eddy activity may be the main cause of the whole eastward shift of the NAO pattern during P2/P3.

The result obtained in this paper differs somewhat from some of the previous results (Jung et al. 2003; Luo and Gong 2006; Johnson et al. 2008). In particular, the most important result of the present paper is that the eastward shift of the NAO pattern during P2 and P3 is dominated not only by the eastward displacement of the Atlantic storm-track eddy activity, but also by the meridional shift of the core of the Atlantic jet stream associated with the NAO phase. In previous studies an increase in the strength of the mean westerly winds has been widely recognized to be a main cause of the eastward shift of the center of action of the NAO pattern during P2 (Jung et al. 2003; Luo and Gong 2006). However, in this paper we propose another possible mechanism: that the eastward shift of the Atlantic storm-track activity can result in the eastward shift of the NAO pattern. In fact, a downstream increase in the strength of the mean westerly winds during P2 also basically implies an eastward shift of the Atlantic storm-track eddy activity. Thus, the present study is a complement to the previous studies and can further provide a dynamical explanation for why the spatial structure of the NAO pattern depends on the NAO index (phase) and why the center of action of the NAO pattern, especially the northern center, undergoes an eastward shift during P2.

However, it must be noted that our weakly nonlinear analytical solution cannot account for the dependence of the different tilting of the NAO pattern on the NAO index because of the limitation of some assumptions used in our weakly nonlinear model (Luo et al. 2007b). Although the phase speed of linear Rossby wave in a slowly varying media can interpret the dependence of the spatial tilting of the NAO pattern on the NAO index (phase), the weakly nonlinear analytical solutions used in section 4 need to be further extended so as to explain the spatial tilting of the NAO pattern. This issue deserves further

study. Of course, the mechanism proposed here is based on the results of a simple model, which needs to be further examined in more complex models.

REFERENCES

Benedict, J. J., S. Lee, and S. B. Feldstein, 2004: Synoptic view of the North Atlantic Oscillation. *J. Atmos. Sci.,* **61,** 121–144.

Blackmon, M. L., 1976: A climatological spectral study of 500-mb geopotential height of the Northern Hemisphere. *J. Atmos. Sci.,* **33,** 1607–1623.

Branstator, G., 1983: Horizontal energy propagation in a barotropic atmosphere with meridional and zonal structure. *J. Atmos. Sci.,* **40,** 1689–1708.

Cassou, C., L. Terray, J. Hurrell, and C. Deser, 2004: North Atlantic winter climate regimes: Spatial asymmetry, stationarity with time, and oceanic forcing. *J. Climate,* **17,** 1055–1068.

Cayan, D. R., 1992: Latent and sensible heat flux anomalies over the northern oceans: The connection to monthly atmospheric circulation. *J. Climate,* **5,** 354–369.

Chang, E. K. M., and Y. Fu, 2002: Interdecadal variations in Northern Hemisphere winter storm track intensity. *J. Climate,* **15,** 642–658.

Charney, J. G., and J. G. DeVore, 1979: Multiple flow equilibria in the atmosphere and blocking. *J. Atmos. Sci.,* **36,** 1205–1216.

Cheng, X., G. Nitsche, and J. M. Wallace, 1995: Robustness of low-frequency circulation patterns derived from EOF and rotated EOF analyses. *J. Climate,* **8,** 1709–1713.

Feldstein, S. B., 2003: The dynamics of NAO teleconnection pattern growth and decay. *Quart. J. Roy. Meteor. Soc.,* **129,** 901–924.

——, and C. Franzke, 2006: Are the North Atlantic Oscillation and the northern annular mode distinguishable? *J. Atmos. Sci.,* **63,** 2915–2930.

Franzke, C., 2009: Multi-scale analysis of teleconnection indices: climate noise and nonlinear trend analysis. *Nonlinear Processes Geophys.,* **16,** 65–76.

——, S. Lee, and S. B. Feldstein, 2004: Is the North Atlantic Oscillation a breaking wave? *J. Atmos. Sci.,* **61,** 145–160.

Haines, K., and P. Malanotte-Rizzoli, 1991: Isolated anomalies in westerly jet streams: A unified approach. *J. Atmos. Sci.,* **48,** 510–526.

Hall, N. M. J., B. J. Hoskins, P. J. Valdes, and C. A. Senior, 1994: Storm tracks in a high-resolution GCM with doubled carbon dioxide. *Quart. J. Roy. Meteor. Soc.,* **120,** 1209–1230.

Hilmer, M., and T. Jung, 2000: Evidence for a recent change in the link between the North Atlantic Oscillation and Arctic sea ice export. *Geophys. Res. Lett.,* **27,** 989–992.

Hoskins, B. J., and D. J. Karoly, 1981: The steady linear response of a spherical atmosphere to thermal and orographic forcing. *J. Atmos. Sci.,* **38,** 1179–1196.

——, and T. Ambrizzi, 1993: Rossby wave propagation on a realistic longitudinally varying flow. *J. Atmos. Sci.,* **50,** 1661–1671.

Hurrell, J. W., 1995a: Decadal trends in the North Atlantic Oscillation: Regional temperature and precipitation. *Science,* **269,** 676–679.

——, 1995b: Transient eddy forcing of rotational flow during northern winter. *J. Atmos. Sci.,* **52,** 2286–2301.

Johnson, N. C., S. B. Feldstein, and B. Trembley, 2008: The continuum of Northern Hemisphere teleconnection patterns and a description of the NAO shift with the use of self-organizing maps. *J. Climate,* **21,** 6354–6371.

Jung, T., and M. Hilmer, 2001: The link between the North Atlantic Oscillation and Arctic sea ice export through Fram Strait. *J. Climate,* **14,** 3932–3943.

——, ——, E. Ruprecht, S. Kleppek, S. K. Gulev, and O. Zolina, 2003: Characteristics of the recent eastward shift of interannual NAO variability. *J. Climate,* **16,** 3371–3382.

Li, S., W. A. Robinson, M. P. Hoerling, and K. M. Weickmann, 2007: Dynamics of the extratropical response to a tropical Atlantic SST anomaly. *J. Climate,* **20,** 560–574.

Luo, D., 2005: A barotropic envelope Rossby soliton model for block–eddy interaction. Part I: Effect of topography. *J. Atmos. Sci.,* **62,** 5–21.

——, and T. Gong, 2006: A possible mechanism for the eastward shift of interannual NAO action centers in last three decades. *Geophys. Res. Lett.,* **33,** L24815, doi:10.1029/2006GL027860.

——, A. Lupo, and H. Wan, 2007a: Dynamics of eddy-driven low-frequency dipole modes. Part I: A simple model of North Atlantic Oscillations. *J. Atmos. Sci.,* **64,** 3–38.

——, T. Gong, and Y. Diao, 2007b: Dynamics of eddy-driven low-frequency dipole modes. Part III: Meridional displacement of westerly jet anomalies during two phases of NAO. *J. Atmos. Sci.,* **64,** 3232–3248.

——, L. Zhong, R. Ren, and C. Wang, 2010: Spatial pattern and zonal shift of the North Atlantic Oscillation. Part II: Numerical experiments. *J. Atmos. Sci.,* **67,** 2827–2853.

Overland, J. E., and W. Wang, 2005: The Arctic climate paradox: The recent decrease of the Arctic Oscillation. *Geophys. Res. Lett.,* **32,** L06701, doi:10.1029/2004GL021752.

Peterson, K. A., R. J. Greatbatch, J. Lu, H. Lin, and J. Derome, 2002: Hindcasting the NAO using diabatic forcing of a simple AGCM. *Geophys. Res. Lett.,* **29,** 1336, doi:10.1029/2001GL014502.

——, J. Lu, and R. J. Greatbatch, 2003: Evidence of nonlinear dynamics in the eastward shift of the NAO. *Geophys. Res. Lett.,* **30,** 1030, doi:10.1029/2002GL015585.

Rogers, J. C., 1997: North Atlantic storm track variability and its association to the North Atlantic Oscillation and climate variability of northern Europe. *J. Climate,* **10,** 1635–1647.

Sigmond, M., P. C. Siegmund, E. Manzini, and H. Kelder, 2004: A simulation of the separate climate effects of middle-atmospheric and tropospheric CO_2 doubling. *J. Climate,* **17,** 2352–2367.

Thompson, D. W. J., and J. M. Wallace, 1998: The Arctic Oscillation signature in the wintertime geopotential height and temperature fields. *Geophys. Res. Lett.,* **25,** 1297–1300.

Thorncroft, C. D., B. J. Hoskins, and M. E. McIntyre, 1993: Two paradigms of baroclinic-wave life-cycle behaviour. *Quart. J. Roy. Meteor. Soc.,* **119,** 17–55.

Ulbrich, U., and M. Christoph, 1999: A shift of the NAO and increasing storm track activity over Europe due to anthropogenic greenhouse gas forcing. *Climate Dyn.,* **15,** 551–559.

Vautard, R., B. Legras, and M. Deque, 1988: On the source of midlatitude low frequency variability. Part I: A statistical approach to persistence. *J. Atmos. Sci.,* **45,** 2811–2843.

Visbeck, M., H. Cullen, G. Krahmann, and N. Naik, 1998: An ocean model's response to North Atlantic Oscillation-like wind forcing. *Geophys. Res. Lett.,* **25,** 4521–4524.

Walker, G. T., 1924: Correlation in seasonal variation of weather, IX. *Mem. Indian Meteor. Dep.,* **24,** 275–332.

Wallace, J. M., 2000: North Atlantic Oscillation/annular mode: Two paradigms—One phenomenon. *Quart. J. Roy. Meteor. Soc.,* **126,** 791–805.

White, G. H., 1980: On the observed spatial scale of Northern Hemisphere transient motions. *J. Atmos. Sci.,* **37,** 892–894.

Yang, G.-Y., and B. J. Hoskins, 1996: Propagation of Rossby waves of nonzero frequency. *J. Atmos. Sci.,* **53,** 2365–2378.